NUMERICAL DETERMINATION OF AIR EXCHANGE RATE OF AND INSIDE A NATURALLY VENTILATED BARN DEPENDING ON INCOMING WIND ANGLE AND BARN'S LENGTH/WIDTH

Moustapha Doumbia[1], Sabrina Hempel[1], David Janke[1] and Thomas Amon[2]

[1]Leibniz Institute for Agricultural Engineering and Bioeconomy, Department of Engineering for Livestockmanagement, Potsdam, Germany

[2]Institut of Animal Hygiene and Environmental Health, Department of Veterinary Medicine, Freie Universität Berlin, Germany

mdoumbia@atb-potsdam.de, SHempel@atb-potsdam.de, DJanke@atb-potsdam.de, tamon@atb-potsdam.de

ABSTRACT

The air exchange rate is an important parameter in order to evaluate the gas emission of naturally ventilated barns. At the same time, understanding the flow inside such barns helps to investigate the comfort of the animals inside. Yet the air exchange rate is still difficult to assess mainly because of fluctuating influence stimuli such as wind (speed and angle), temperature, barn geometry etc. The main objective of the BELUVA project, financed by the German Research Foundation, is to systematically address those influences. The present study has been carried out in order to investigate the impact of incoming wind angle on the air exchange rate of animal occupied zones of barns with different length/width ratios.

A numerical model with quadrilateral and polyhedral grid cells (hybrid mesh) was set up in ANSYS Workbench. The numerical domain was divided into blocks for better meshing controls and quality. The influence of the roughness height was studied as well to reduce the numerical error related to the non-horizontal homogeneity of the velocity profile downstream.

Going from this numerical model, the air exchange rate of the whole barn and of the animal occupied zones inside has been determined and compared for different cases. The cases distinct themselves by three different incoming wind angles (0 °, 45 ° and 90 °), three different barn's length (L) / barn's width (W) (L/W=2,3,4) ratio and three different velocity magnitudes (1, 3 and 5 m s^{-1}).

The results show that the influence of the velocity incident angle on the air exchange rate of the overall barn and the animal occupied zones inside can be classified in types at least for the 0 ° and 90 ° incident angles. This, depending on the *L/W* ratio, gives important information about the height of the local in air exchange rate.

Keywords*:* air exchange rate, CFD simulation, meshing strategy, animal occupied zone.

1. INTRODUCTION

The implementation of computational fluid dynamics (CFD) in the study of barns has been growing in the recent years (Rong et al., 2016). The purposes, however, are totally different. For example, Wu et al., 2012 used CFD technics to evaluate air exchange rate measurement methods. Bjerg et al., 2013 and Fiedler et al., 2014 analyzed the gas emission from barns while Norton et al., 2008 investigated the influence of openings on the animal thermal comfort.

But still a lot has to be done to fully comprehend the influence of the different factors on the flow outside and inside a barn. Indeed, there are geometrical parameters such as the length/width (*L/W*) ratio of a barn that has yet to be taken into account. A barn design is relatively simple compared to other buildings. This simplicity allows the farmers to build the barn depending on the number of animals they possess, which results in a high variety of *L/W* ratio.

The paper should be considered as a second part of the paper published in Ciosta conference (Doumbia et al., prediction of the local air exchange rate in animal occupied zones of a naturally ventilated barn). While the latter paper focuses on the CFD validation and results analysis, this paper deals mainly with the numerical pre-studies aspect and preparation that was undergone to achieve reliable results.

2. NUMERICAL SIMULATION

All the numerical investigations were done in wind tunnel of scale (1:100).

2.1 Methods Barn details: Domain size and dimension

In figure 1 the dimensions of the computational domain are presented as well as the mesh refinement box with H = 114 mm (barn's height) and W = 342 mm (barn's width) as reference lengths. The dimensions were chosen to be large enough so that the walls do not impact the main flow. For the same reasons the side walls were used as the velocity inlets, see Figure 2 for the full list boundary conditions. The animal occupied zones had the following dimensions: H_AOZ = 30 mm, L_AOZ = L/4, W_AOZ = W/4.

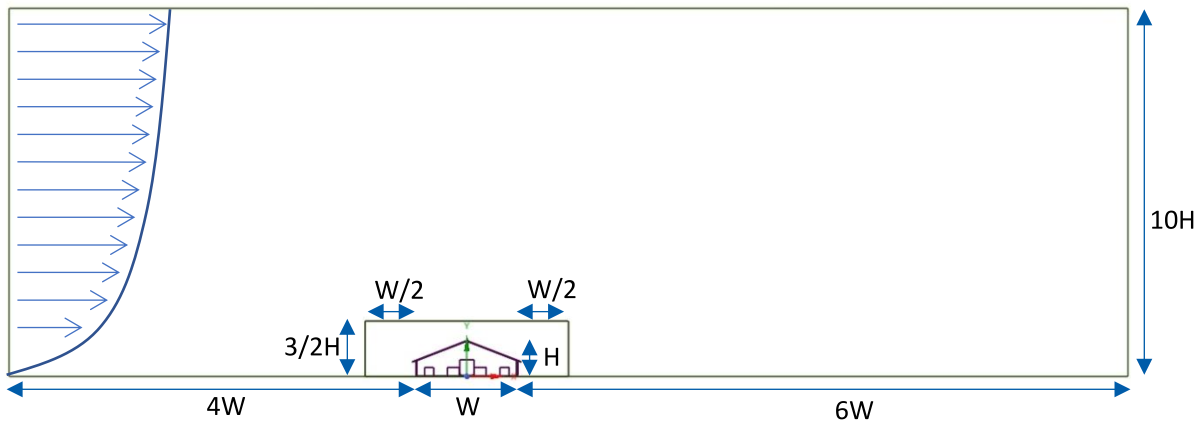

Figure 1. Dimensions of the numerical domain

Along with the velocity profile at the domain inlet, the profile for *k* (the turbulent kinetic energy) and *ε* (the turbulent dissipation rate) were implemented as well. The parameters *k* and *ε* were obtained from the wind tunnel measurement data of the turbulent intensity I using the following equations described in ANSYS Fluent User's Guide:

$$k = \frac{3}{2}\left(U_{avg}I\right)^2$$

$$\epsilon = \frac{k^{3/2}}{l}$$

where U_{avg} and l are the average velocity and the turbulent length scale respectively.

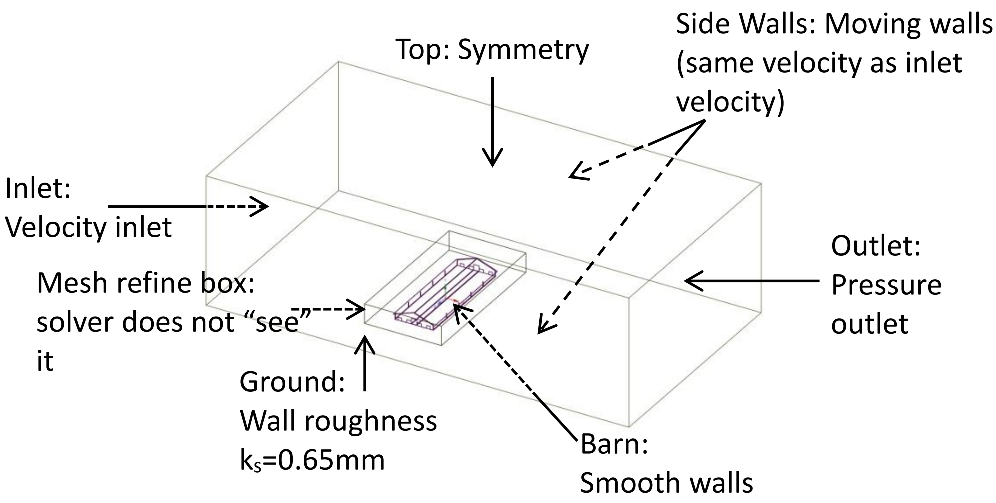

Figure 2. Boundary conditions

For the studied cases the k-ε realizable turbulence model was selected as recommended by Fluent (Lanfrit et al., 2005) for external dynamic flows. The pressure-based solver was preferred over the density-based since the flow is supposed to be incompressible, steady, with gas transport and isotherm (no energy source). In addition, the coupled scheme was selected since, from our experience and Fluent theory guide, it offers better performance and a more "robust and efficient single-phase implementation for steady flows" over the segregated schemes.

2.2 Meshing strategy

The computational domain was divided into blocks to achieve a better mesh control (cf: figure 3). The resulting hybrid mesh is a combination of tetrahedral cells (barn's block only) and quadrilateral cells (all other blocks), which puts the effort of mesh quality improvement only to the barn's box.

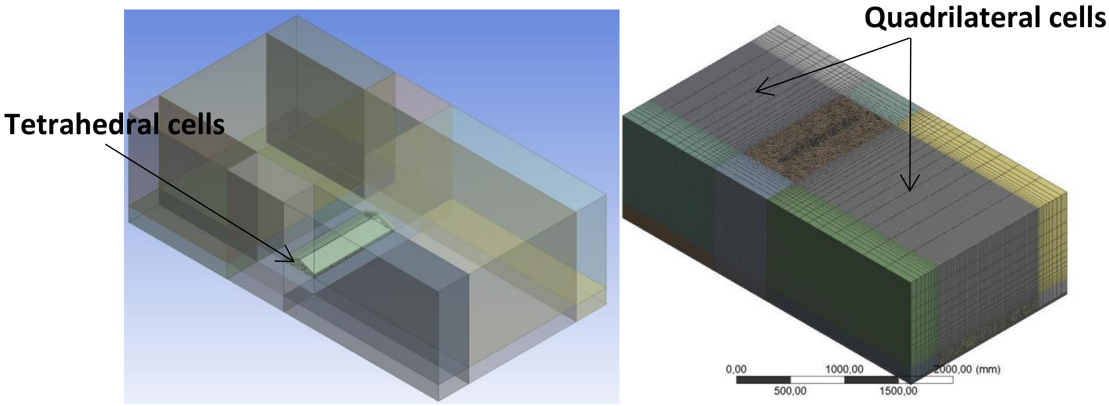

Figure 3. Computational domain divided into blocks

Tetrahedral mesh was chosen for the barn's box since this type of mesh is able to capture complex geometry details like sharp angles and small segments. Information about the cells number and quality for each *L/W* ratio obtained from Ansys Meshing are listed in table 1. Referring to Ansys meshing user guide, mesh quality metrics like the skewness, which evaluates how close to ideal a cell is, is important since it affects the simulation accuracy and stability. Based on table 2, the average skewness of the domain for all *L/W* ratios is evaluated as almost excellent.

Moreover, a Ansys Fluent technique, consisting of converting tetrahedral cells to polyhedral, was used to further reduce the total cell number up 40 % and thus reduce computational time.

Table 1. Cells number and mesh average skewness for each *L/W* ratio

L/W ratio	2	3	4
Cells number (in million)	12.09	17.18	21.66
Average skewness	0.256	0.254	0.253

Table 2. Skewness mesh metrics spectrum

Cell quality	Degenerate	Bad	Poor	Fair	Good	Excellent	Equilateral
Value of skewness	1	1 < - 0.9	0.9 – 0.75	0.75 – 0.5	0.5 – 0.25	0.25 - > 0	0

2.3 Roughness height k_s

One of the main difficulties in modeling flow in atmospheric boundary layer (ABL) (1:200 m in real scale) is to maintain the horizontal uniformity of the velocity profile in the flow direction. And one of the important parameters impacting the uniformity is the roughness height k_s of the numerical domain, which is supposed to simulate the obstacles of terrain surrounding the object under investigation (Bocken and al, 2008). In order to find the right k_s corresponding to the wind tunnel setup and arrangement and at the same time minimizing the non-uniformity of the velocity profile, a pre-study was done in an empty domain. In detail the equation given in Durbin et al., 2001 and Blocken et al, 2007 was solved to obtain the mathematical k_s:

$$U(y) = U_{ref} \times \frac{\ln\left(\frac{y}{y_0}\right)}{\ln\left(\frac{y_{ref}}{y_0}\right)}$$

In Ansys Fluent the roughness is defined as:

$$k_s = \frac{9.793\, y_0}{C_s}$$

Where *U(y)* is the wind velocity at the height *y*, U_{ref} a reference velocity at a reference height y_{ref} and C_S a roughness constant with a standard value of 0.5 (Blocken et al, 2007). Then giving velocity profile from the measurement data at the inlet of the domain, simulations were performed with different k_s values. The relative discrepancies of the velocity at different distances from the inlet compared with the inlet velocity were evaluated and are shown in figure 4. In the domain of interest (the first 4 m > 11 *W*), the errors were the smallest for ks = 0.00065 m.

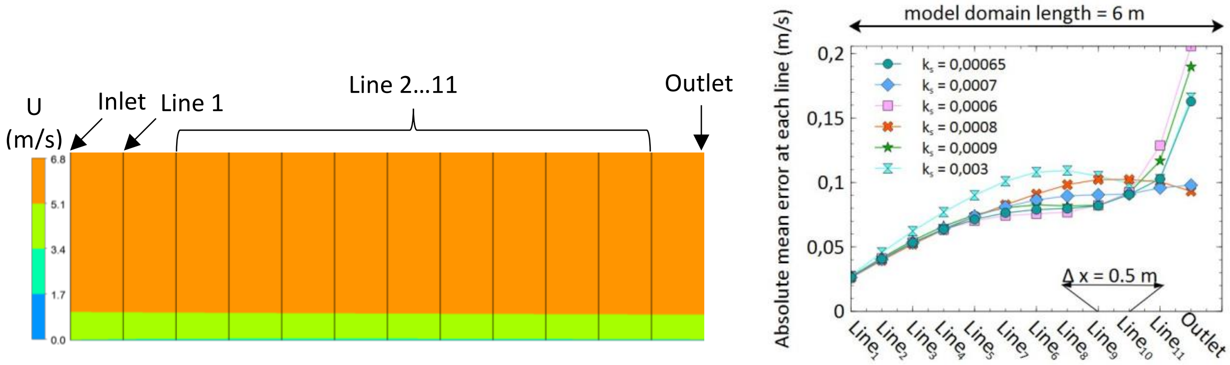

Figure 4. Relative velocity discrepancies along the domain compared to inlet velocity

3. Results and Discussion

After validation of the numerical model with the wind tunnel measurements, the impact of *L/W* (= 2, 3, 4), velocity magnitude at the barn's inlet U (= 1, 3, 5 m s^{-1}) and incident velocity angle (0 °, 45 °, 90 °) on the air exchange rate of the whole barn (AER_{Barn}) and the animal occupied zone (AER_{AOZ}) was investigated. The simulations were done with Reynolds number Re > 80000 to ensure fully developed turbulence. The AER for the individual AOZs and the barn are presented in Figure 5 in s^{-1} (s^{-1} instead of h^{-1} since the calculations has been done in scale dimension 1:100).

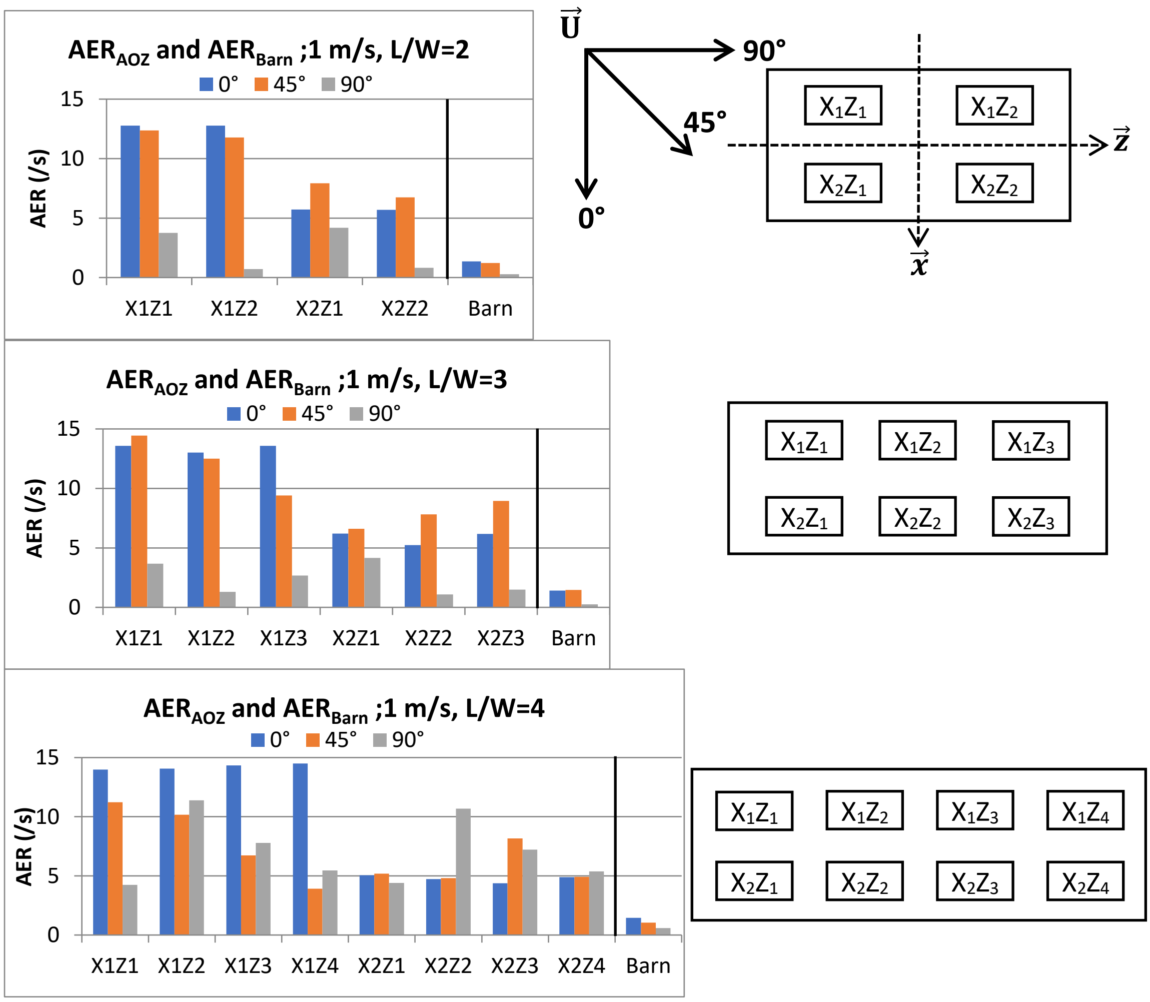

Figure 5. AER_{Barn} and AER_{AOZ}s for the 1 m s^{-1} case; Right: AOZs positions

From figure 5 the main findings can be summarized as follows:

- The AER_{Barn} alone is unable to provide valuable information about the changes inside.
- Each velocity incident case demonstrates a distinct pattern independent of the *L/W* ratio.
- For 0 ° incident angle, the AER_{AOZ} of the second line (X_2Z_b, b=1..*L/W*) is around half of the AER_{AOZ} of the first line (X_1Z_b, b=1..*L/W*).
- For 90 ° incident angle, considering the Z direction as symmetric axis, the AER_{AOZ} of one side (AER_{X1Zi}) have almost the same values as the one of the other side (AER_{X2Zi}).
- The 45 ° incident angle is the most unpredictable case, in the first line (X_1Z_i) values are decreasing from Z_i to Z_{i+1}. In the second line (X_2Z_i) the pattern changes with the *L/W* ratio.

The same can be observed for the other tested velocity magnitudes as well.

5. Conclusions

This paper focuses on the numerical modelling preparation for the study of AER in barns depending on various parameters. A meshing strategy by blocks was used in order to have better control and reduced cells number. The roughness k_s = 0.00065 m was found to minimize the numerical error in the ABL. Finally, it was shown that the influence of the velocity incident angle on the air exchange rate of the animal occupied zones inside the barn cannot be ignored. It can be classified in typical pattern at least for the 0 ° and 90 ° incident angles. This allows obtaining important information on the height of the local air exchange rate depending on the position inside the barn.

Further work will take into account the convection and gas flow in a real sized barn in the pursuance of a better comprehension of AER dependency.

References

Rong, L. (2001) 'Mechanisms of natural ventilation in livestock buildings: Perspectives on past achievements and future challenges', Biosystems engineering. doi: 10.1016/j.biosystemseng.2016.09.004.

Wu, W. (2012) 'Evaluation of methods for determining air exchange rate in a naturally ventilated dairy cattle building with large openings using computational fluid dynamics (CFD), Atmospheric Environment, 63, pp. 179 to 188. doi: 10.1016/j.atmosenv.2012.09.042.

Bjerg, B. (2013) 'Modelling of ammonia emissions from naturally ventilated livestock buildings. Part 3: CFD modelling', Biosystems engineering, 116, pp. 259 to 275. doi: 10.1016/j.biosystemseng.2013.06.012.

Norton, T. (2008) 'Assessing the ventilation effectiveness of naturally ventilated livestock buildings under wind dominated conditions using computational fluid dynamics', Biosystems engineering, 103, pp. 78 to 99. doi: 10.1016/j.biosystemseng.2009.02.007.

Fiedler, T. (2008) 'Spatial distribution of air flow and CO2 concentration in a naturally ventilated dairy building', Environmental Engineering and Management Journal, 13, 9, 2193-2200.

Blocken, B. (2017) 'CFD simulation of the atmospheric boundary layer: wall function problems', Atmospheric Environment. doi: 10.1016/j.atmosenv.2006.08.019.

Lanfrit, M. (2005) 'Best practice guidelines for handling Automotive External Aerodynamics with FLUENT'.

ANSYS Fluent User's Guide, version 18.1 (2017)

ANSYS Fluent Theory Guide, version 18.1 (2017)